www.czasopisma.pan.pl PAN www.journals.pan.pl

ARCHIVES of FOUNDRY ENGINEERING

DE GRUYTER OPEN

ISSN (2299-2944)
Volume 17
Issue 4/2017

DOI: 10.1515/afe-2017-0138

Published quarterly as the organ of the Foundry Commission of the Polish Academy of Sciences

103 – 108

Properties of the Inconel 713 Alloy Within the High Temperature Brittleness Range

K. Łyczkowska [a, *], J. Adamiec [a], R. Jachym [b], K. Kwieciński [b]
[a] Institute of Materials Science, Silesian University of Technology
Krasińskiego 13, 40-019 Katowice, Poland
[b] Welding Institute
Bl. Czeslawa 16-18, 44-100 Gliwice
* Corresponding author: Email address: katarzyna.lyczkowska@polsl.pl

Received 10.04.2017; accepted in revised form 03.08.2017

Abstract

Nickel-based alloys are widely used in industries such as the aircraft industry, chemicals, power generation, and others. Their stable mechanical properties in combination with high resistance to aggressive environments at high temperatures make these materials suitable for the production of components of devices and machines intended for operation in extremely difficult conditions, e.g. in aircraft engines. This paper presents the results of thermal and mechanical tests performed on precision castings made of the Inconel 713C alloy and intended for use in the production of low pressure turbine blades. The tests enabled the determination of the nil strength temperature (NST), the nil ductility temperature (NDT), and the ductility recovery temperature (DRT) of the material tested. Based on the values obtained, the high temperature brittleness range (HTBR) and the hot cracking resistance index were determined. Metallographic examinations were conducted in order to describe the cracking mechanisms. It was found that the main cracking mechanism was the partial melting of grains and subsequently the rupture of a thin liquid film along crystal boundaries as a result of deformation during crystallisation. Another cracking mechanism identified was the DDC (Ductility Dip Cracking) mechanism. The results obtained provide a basis for improving precision casting processes for aircraft components and constitute guidelines for designers, engineers, and casting technologists.

Keywords: Thermal and mechanical tests, Inconel 713C, Gleeble, High temperature brittleness range

1. Introduction

Nickel-based alloys are widely used in various industries where the required material properties include heat resistance and creep resistance. Nickel-based alloys are used for precision castings and high-pressure castings [1]. The most frequent defects in nickel-based alloy castings are misruns, micro-shrinkage, and cracks. In the case of castings having complex shapes, the number of defective castings can exceed 10% [2]. Defects forming during the casting process and during service can be repaired by welding and pad welding. Unfortunately, the technologies employed to repairs of cast components do not always produce the desired results, which often renders production unprofitable. The main reason for the disqualification of complete structures or individual castings from use are pores and cracks that form during the casting process [2]. The feasibility of repairing components made of nickel-based alloys using welding methods depends crucially on the weldability of those alloys. Weldability is defined as the ability of a material to form permanent joints made by welding, with the joints satisfying certain requirements [3]. The greatest problem in welding and pad welding of nickel-based alloys is their susceptibility to hot cracking during weld crystallization [4,

5]. Such cracks result from phenomena occurring in the so-called high temperature brittleness range (HTBR)(Fig. 1)[6-9].

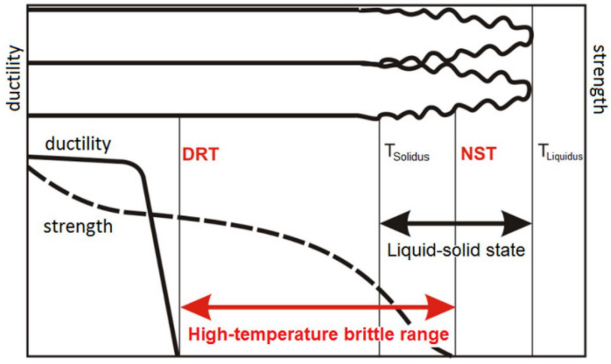

Fig. 1. High temperature brittleness range determining hot cracking in welds [9]

The HTBR is defined as the range between the temperature at which a metal has acquired mechanical strength during crystallization and the temperature at which the metal is capable of undergoing plastic deformation (Fig. 2) [5].

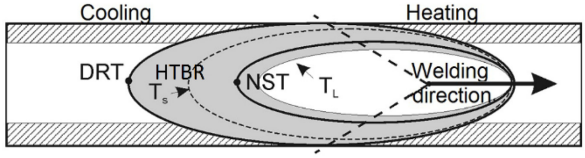

Fig. 2. Model of the high-temperature brittleness range in a weld pool [5]

During the welding process, hot cracks can form within the HTBR which do not appear outside that range. Hot cracks, also referred to as crystallization cracks, are defined as cracks forming during crystallization. They form as a result of rupture of bridges connecting crystals (Fig. 3) [5] as a result of rupture of a thin liquid film, or along the grain boundaries of phases incapable of transmitting deformations related to wed shrinkage [9-11].

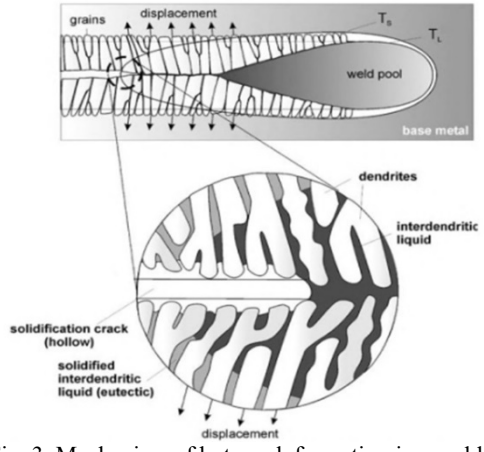

Fig. 3. Mechanism of hot crack formation in a weld [5]

The HTBR is influenced by three groups of factors:

- metallurgical (chemical composition, metallurgical reactions, and the welded joint structure),
- technological (welding parameters determining the quantity of heat supplied to the material),
- design-related (the shape of the casting and its specific rigidity).

Thus, it can be stated that the weldability of nickel-based casting alloys depends on design, technological, ale metallurgical factors that affect the susceptibility of a material to hot cracking in the HTBR (Fig. 4) [8].

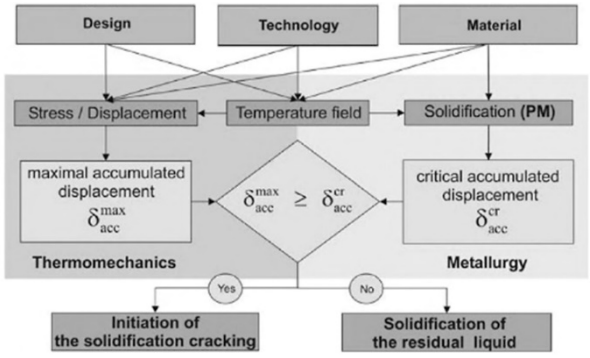

Fig. 4. Phenomenological interrelation between hot cracking criteria and factors affecting susceptibility to cracking [8]

In order to determine the effect of metallurgical and technological factors on the breadth of the high temperature brittleness range, the properties of Inconel 713C were tested using the Gleeble 3500 physical simulation and thermal and mechanical testing system [12]. The studies enabled describing the phenomena occurring during material crystallization and under the simulated non-equilibrium conditions of the welding process. The basic temperatures within the HTBR were determined:

- *DRT — Ductility Recovery Temperature,*
- *NDT — Nil Ductility Temperature,*
- *NST — Nil-Strength Temperature.*

This enabled the determination of the HTBR — Inconel 713C [11, 12].

2. Materials and methodology

The material used in the tests was the polycrystalline nickel-based Inconel 713C alloy. The precision castings were made at Consolidated Precision Products Poland Sp. z o.o. The test specimens were provided in the form of truncated cones measuring 95x25x13 mm (Fig. 5). The chemical composition was verified by X-ray diffraction, with the use of an XRF NitonHLt 898W analyser. The results of the analysis are shown in Table 1.

Table 1.
Chemical composition on Inconel 713C - XRF method (wt.-%) [11]

Alloy	Ni	Cr	Al	Mo	Nb	Zr	W	Cu	Co + Ta	Fe	Mn
Inconel 713C (XRF)	70.38	13.29	5.8	4.4	2.1	0.04	0.3	0.47	1.92	0.36	0.08
Material Specification	other	12-14	5.5-6.5	3.8-5.2	< 2.5	<0.15	-	< 0,5	1.8-2.8	< 2.5	<0.25

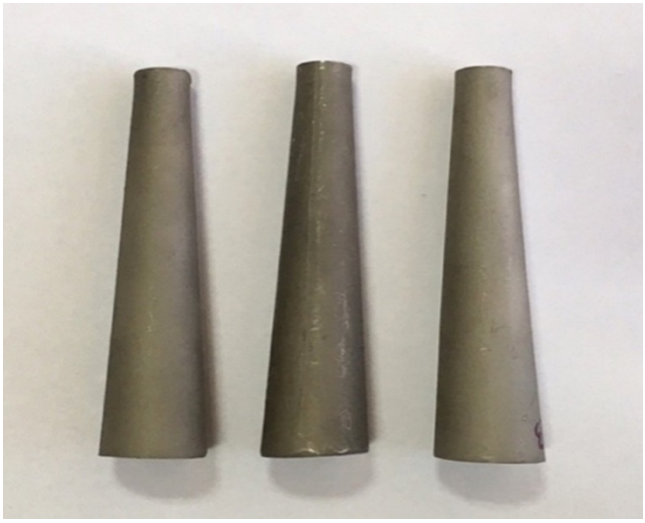

Fig. 5. Test specimens made of Inconel 713C

The influence of metallurgical factors on the weldability of the alloy was determined by differential thermal analysis (DTA), which enabled the determination of the actual solidus and liquidus temperatures during heating and cooling (Table 2). The results obtained were used for tests on the Gleeble 3500 simulator. The tests were carried out at the Welding Institute in Gliwice.
The tests were conducted on cylindrical specimens measuring Ø 6×90 mm (Fig. 6a). A type S thermocouple was used to heat the test material. The specimens were fixed in copper grips (Fig. 6b), heated in vacuum at a rate of 20°C/s up to the solidus temperature, and finally allowed to cool freely. The NST, NDT, and DRT were determined for the material tested. The results obtained enabled the determination of the hot cracking resistance index $R_f = \frac{TL-NDT}{NDT}$ (where *TL* is the liquidus temperature) and the determination of the high temperature brittleness range, here understood as the difference between the NST and the DRT.

Table 2.
Heating and cooling conditions during the differential thermal analysis and the characteristic temperatures of the process

Heating temperature [°C]	Heating/ cooling rate [°C/min]	Atmos-phere [%]	Gas flow rate [l/h]	Furnace thermocouple type	Temperature Solidus [°C]	Temperature Liquidus [°C]
1200	10	Ar 99.999	1.45	S type (Pt-Rh 10%)	1263	1343

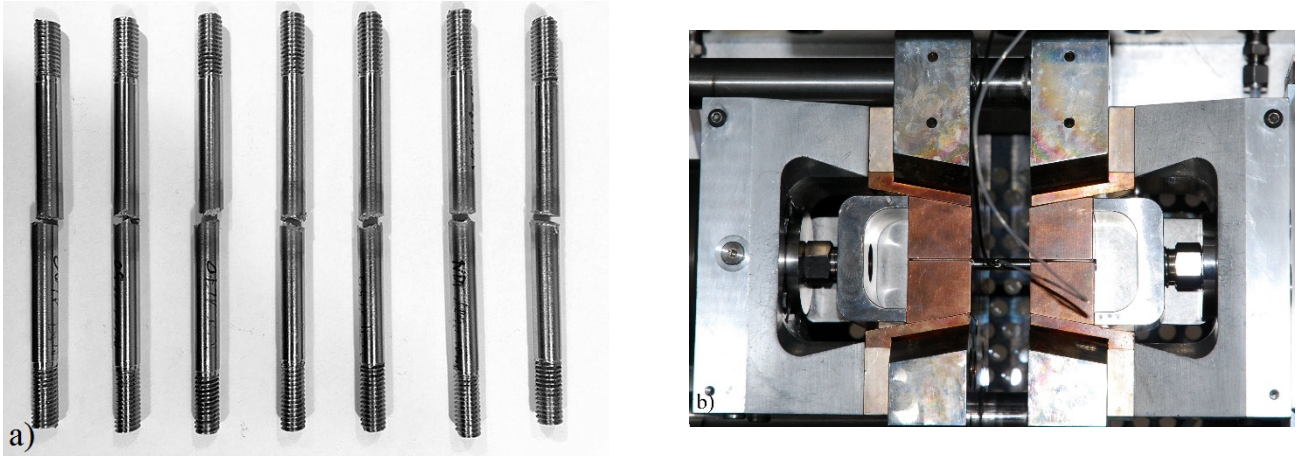

Fig. 6. Determination of the DRT: a) Samples for testing, b) view of the Gleeble 3500 simulator chamber with a specimen fixed in it

The tests were complemented by observations of metallographic cross-sections under an SZX9 stereoscopic microscope (SM) (Fig. 7a, 8a, and 9a),; an Olympus GX71 light microscope (LM), at magnifications of up to 200x (Fig. 7b, 8b, and 9b), and under a JEOL JCM-6000 Neoscope II scanning electron microscope (SEM) (Fig. 7c,d, 8c, d, 9c, d). Images were recorded in the secondary electron mode, at a voltage accelerating the electron beam to 15keV. The examinations were complemented by an EDS microanalysis of the chemical composition.

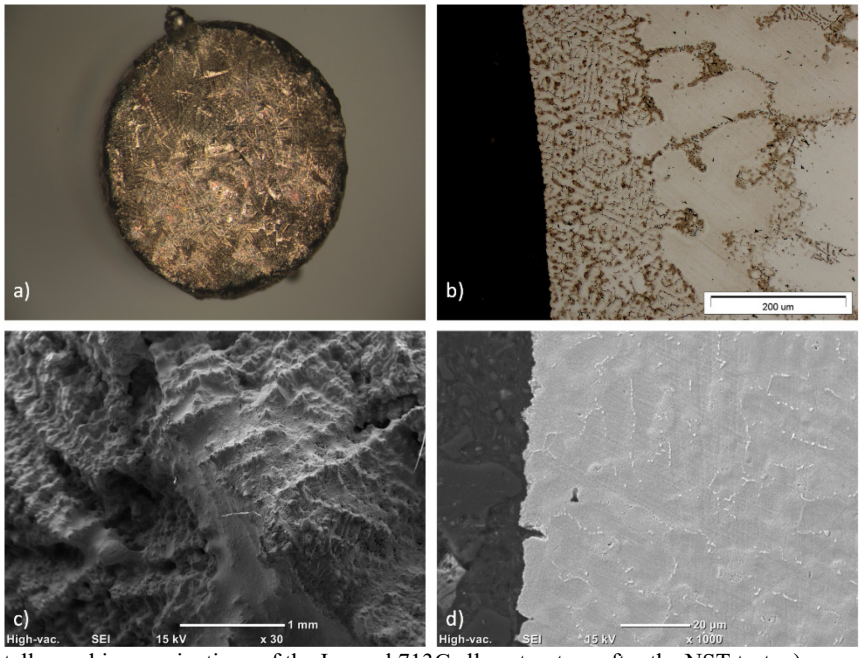

Fig. 7. Results of the metallographic examinations of the Inconel 713C alloy structure after the NST test: a) macrostructure of the fracture area, SM, b) microstructure at the fracture line, LM, c) dendritic structure of the fracture area, SEM, d) microstructure at the fracture line, SEM

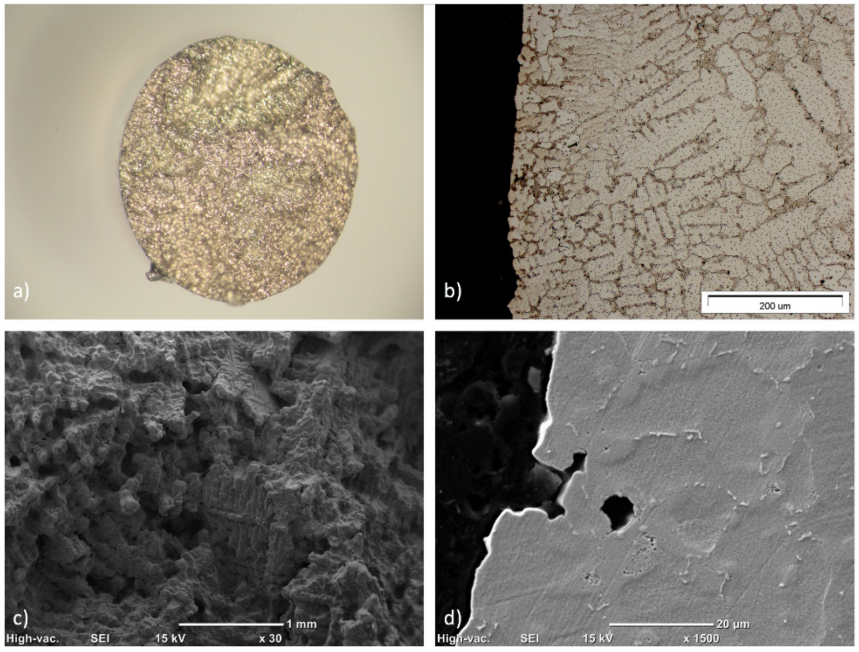

Fig. 8. Results of the metallographic examinations of the Inconel 713C alloy structure after the NDT test: a) macrostructure of the fracture area, SM, b) microstructure at the fracture line, LM, c) dendritic structure of the fracture area, SEM, d) microstructure at the fracture line, SEM

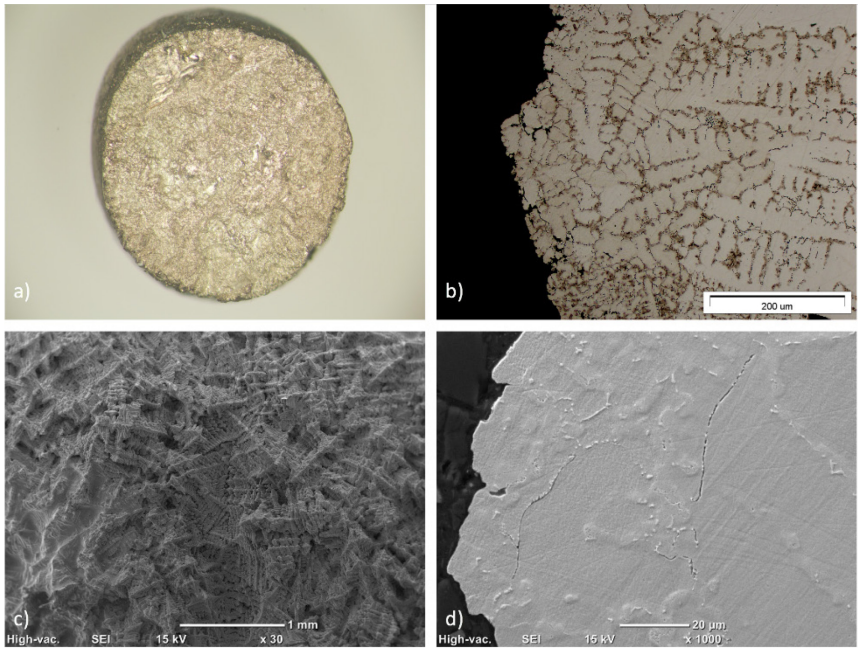

Fig. 9. Results of the metallographic examinations of the Inconel 713C alloy structure after the DRT test: a) macrostructure of the fracture area, SM, b) microstructure at the fracture line, LM, c) dendritic structure of the fracture area, SEM, d) microstructure at the fracture line, SEM

3. Test results

The purpose of the study was to evaluate the influence of the Inconel 713C structure on the hot cracking mechanism. The nil ductility temperature during heating and the ductility recovery temperature during cooling were also determined for the alloy.

For the purposes of the study, the nil ductility temperature (NDT) was defined as the temperature at which the percentage reduction in area at fracture was smaller than 1%. The ductility recovery temperature (DRT) was defined as the temperature at which the percentage reduction in area at fracture was larger than 1%. Both experiments were conducted at a deformation rate of 20 mm/s. The changes in strain and temperature in Inconel 713C as a function of time are shown in Fig. 10a,b.

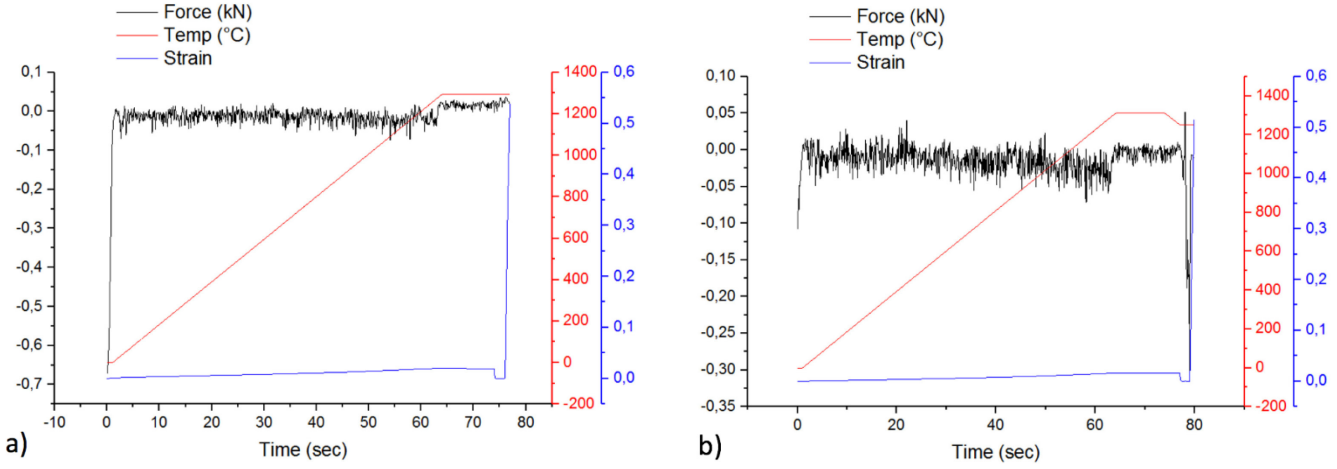

Fig. 10. Changes in strain and temperature in an Inconel 713C specimen: a) NDT test, b) DRT test

Table 3 shows the DRT and NST temperature, mechanical properties (RA) at specific temperatures, and calculations of the HTBR breadth (being the difference between the NST and the DRT).

Table 3.
DRT and NST test parameters and results for the Inconel 713C alloy

Specimen No.	V_0 [mm/s]	RA [%]	NST [°C]	DRT [°C]	HTBR [°C]	Δ HTBR [°C]
1	20	1.1	1290	1250	1250–1290	40

4. Result analysis and summary

Based on the DTA test results, the solidus temperature of Inconel 713C was determined to be 1262 °C and the liquidus temperature was determined to be 1343 °C. The results obtained were the basis for the determination of the nil ductility temperature, the ductility recovery temperature, and the nil strength temperature, which was achieved using the Gleeble 3500 physical simulation and thermal and mechanical testing system. It was found that the NST of Inconel 713C was 1290 °C.
The analysis of the microstructure revealed fragmentation of dendrites along the entire length of the fracture line. As a result of partial melting in the interdendritic spaces, a large number of fine carbides precipitated in the interdendritic spaces, forming characteristic clusters.
Deeper into the material, dendrites were much larger in comparison with those observed in the fracture area, and carbides in the interdendritic spaces formed the so-called Chinese script (Fig. 7c). The SEM image obtained showed that a considerable proportion of carbides dissolved along grain boundaries. This phenomenon has an adverse effect on the strength of materials. In each specimen, discontinuities appeared over the entire fracture surface (Fig. 7d).
During the NDT tests, the specimens were heated within the temperature range of 1280–1330 °C, with each next specimen being heated at a temperature higher by 10° in comparison with the previous specimen, and subsequently stretched with a force of 0.1 kN (Table 4) (Fig. 10a,b). The NDT was defined as the temperature at which the deformation at fracture was smaller than 1%.

Table 4.
NDT test parameters and results for the Inconel 713C alloy

Specimen No.	V_0 [mm/s]	RA [%]	NDT [°C]	R_f
1	20	0.9	1280	0.049
2		0.87	1285	0.045
3		0.88	1290	0.041
4		0.92	1295	0.037
5		0.94	1300	0.033

The visual examination of the microstructure revealed a dendritic arrangement typical of nickel-based casting alloys. The dendrite size slightly decreased towards the fracture line in comparison with the NST. Discontinuities were also observed in the structure examined. The DRT was found to be 1250°C, with the percentage reduction in area being 1.1%. During the examination of the alloy structure, cracks propagating along dendrite arm boundaries were identified. In each specimen, hot cracks appeared over the entire surface examined.
The NDT, NST, and DRT temperatures measured during the tests were the basis for the determination of the range within which the alloy studied is brittle. It can be concluded that the HTBR for the Inconel 713C alloy is very narrow — only 40 °C.

Acknowledgements

The study was funded as part of the Applied Research Programme financed by the National Centre for Research and Development, project title: “Advanced Casting Technologies – INNOCAST”, contract No.: INNOLOT/I/8/NCBR/2013.

References

[1] DuPoint, J.N., Lippold, J.C., Kiser, S.D. (2009). *Welding metallurgy and weldability of nickel-base alloys*. New Jersey - USA: Wiley.
[2] Chodorowski, J., Ciszewski, A., Radomski, T. (2003). *Aeronautical materials*. Warszawa - Polska: Oficyna Wydawnicza Politechniki Warszawskiej. (in Polish).
[3] Pilarczyk, J. (eds.) (2003). *Engineer's Guide – Welding. Vol 1*. Warszawa - Polska: Wydawnictwo Naukowo-Techniczne. (in Polish).
[4] Tasak, E. & Ziewiec, A. (2007). Cracking of welds in the solidification process. *Przegląd spawalnictwa*. 1, 14-18. (in Polish).
[5] Polshikhin, V., Prokhodovsky, A., Makhutin, M., Zoch, H. (2005). Integrated mechanical-metallurgical approach to modeling of solidification cracking in welds, In Bollinghaus T., Herold H. (Eds.) Hot cracking phenomena in welds, 223-244. Heidelberg - Germany: Springer.
[6] Zupaniĉ, F., Bonĉina, T., Kiržman, A., Tichelaar, F.D. (2001). Structure of continuously cast Ni-based superalloy Inconel 713C. *Journal of Alloys and Compounds*. 329, 290-297. DOI 10.1016/S0925-8388(01)01676-0.
[7] Tasak, E. (2008). *Welding metallurgy*. Kraków - Polska: Wyd. JAK. (in Polish).
[8] Herold, H., Pchennikov, A., Steitenberger, M. (2005). Influence of deformation rate of different test on hot cracking formation, In Bollinghaus T., Herold H. (Eds.) Hot cracking phenomena in welds, 328-346. Heidelberg - Germany: Springer.
[9] Yeshuang, W., Baode, S., Qudong, W., Yanping, Z. & Wenjiang, D. (2002) An understanding of the hot tearing mechanism in AZ91 magnesium alloy. *Materials Letters*. 53(1-2), 35-39. DOI: 10.1016/S0167-577X(01)00449-9.
[10] Acton, Q.A. (Eds.) (2013). Advances in Machine Learning Research and Application, Georgia - USA: Scholarly Editions.
[11] Davis, J.R. (2000). Nickel, Cobalt, and Their Alloys. Ohio - USA:ASM International.
[12] Gleeble 3800 Applications, Welding Process Simulation. (2000). New York – USA.